Spatiotemporal Temperature Variability over the Tibetan Plateau: Altitudinal Dependence Associated with the Global Warming Hiatus

DANLU CAI

Institute of Remote Sensing and Digital Earth, Chinese Academy of Sciences, Beijing, China

QINGLONG YOU

Key Laboratory of Meteorological Disaster of Ministry of Education, and Collaborative Innovation Center on Forecast and Evaluation of Meteorological Disasters, Nanjing University of Information Science and Technology, Nanjing, China

KLAUS FRAEDRICH

Max-Planck-Institute for Meteorology, Hamburg, Germany

YANNING GUAN

Institute of Remote Sensing and Digital Earth, Chinese Academy of Sciences, Beijing, China

(Manuscript received 27 April 2016, in final form 13 October 2016)

ABSTRACT

The recent slowdown in global warming has initiated a reanalysis of temperature data in some mountainous regions for understanding the consequences and impact that a hiatus has on the climate system. Spatiotemporal temperature variability is analyzed over the Tibetan Plateau because of its sensitivity to climate change with a station network updated to 2014, and its linkages to remote sensing–based variability of MODIS daytime and nighttime temperature are investigated. Results indicate the following: 1) Almost all stations have experienced a notable warming in the time interval 1961–2014, with most obvious warming in winter, which depends on the selected time intervals. 2) There is no clear shift from a predominant warming to a near stagnation during the most recent period (2001–present). 3) Uniform altitudinal dependence of temperature change trends could not be confirmed for all regions, time intervals, and seasons, but sometimes an altitude threshold around 3 km is apparent. 4) Most of the meteorological stations are associated with MODIS temperature warming pixels, and thus regional cooling is missing when considering only the locations of meteorological stations. In summarizing, previous studies based on station observations do not provide a complete picture for the temperature change over the Tibetan Plateau. Remote sensing–based analyses have the potential to find early signals of regional climate changes and assess the impact of global climate changes in complex regional, seasonal, and altitudinal environments.

1. Introduction

Global significant increasing warming trend since the industrial revolution (Hartmann et al. 2013) is likely to be punctuated by decadal periods of weaker or stalled warming or even cooling (Amaya et al. 2015; Easterling and Wehner 2009; England et al. 2014; Foster and Rahmstorf 2011; Kosaka and Xie 2013). The observed apparent stagnation of surface temperature warming trend, as documented by, for example, the HadCRUT4 dataset, is widely referred to as a hiatus (Trenberth and Fasullo 2013). One of the examples of hiatus occurs in a period from the 1940s to the 1970s, followed by a resumed trend of overall upward surface air temperature from 1975 to 2000, particularly with a decade of accelerated warming from about 1975 to 1985 (England et al. 2014). The current hiatus since around 2001 to the present is not predicted by climate models (Fyfe et al. 2013; Tollefson 2014) and a deeper understanding of its underlying causes is necessary (Gleisner et al. 2015).

Uncertainty remains about the mechanisms driving the transition from a rapid warming period to a global warming hiatus period (Amaya et al. 2015; Gleisner

Corresponding author e-mails: Yanning Guan, guanyn@radi.ac.cn; Danlu Cai, caidl@radi.ac.cn

DOI: 10.1175/JCLI-D-16-0343.1

© 2017 American Meteorological Society

et al. 2015), spurring debate regarding its underlying causes. Otto et al. (2013) suggest that climate sensitivity may have been overestimated. Cowtan and Way (2014) and Karl et al. (2015) point to incomplete global coverage of the observational temperature data and a possible data bias leading the underestimation of the warming rate. Others suggest that internal natural decadal climate variations and the hiatus originate from the Pacific and Atlantic Ocean from where they induce temperature and precipitation response on regional and global scales (Dai 2013; Dai et al. 2015; Dong and Dai 2015; Steinman et al. 2015; Watanabe et al. 2014). Other physical explanations include changes in solar variability, deep ocean heat uptake, and stratospheric or tropospheric circulation (Meehl et al. 2014; Santer et al. 2014; Schmidt et al. 2014; Tollefson 2014). Much of the evidence suggests that the surplus energy has been stored in the world's oceans (Guemas et al. 2013; Meehl et al. 2011), in particular the equatorial Pacific (England et al. 2014; Kosaka and Xie 2013; Meehl et al. 2014; Trenberth and Fasullo 2013).

Since hiatus periods are likely to disrupt warming trends (Hansen et al. 2011) and therefore redistribute global and regional water resources (Chen et al. 2015), increased attention has been paid to the causes. But it is also important to improve our understanding of the impact that a hiatus has on the climate system and its extent. A linkage between the current hiatus in global warming and North American drought (encompassing regions from the western Great Plains to the U.S. West Coast since around the year 2000) is suggested by Delworth et al. (2015). Vuille et al. (2015) notice that the recent hiatus in global warming is likely to be reflected in Andean temperature, but highly depends on elevation. Coastal regions of Andean experience cooling, while higher elevations continue to warm. That is why Andean glaciers continue to retreat faster than at any time since they reached their neoglacial maximum extent (Rabatel et al. 2013), which has spurred a reanalysis of temperature data in high mountainous regions (Schauwecker et al. 2014).

The Tibetan Plateau (TP), with its unique climatic and biogeographical environment, is defined as the center of the ''Third Pole'' and is also highly sensitive and vulnerable to climate change and to anthropogenic activities (Cai et al. 2014; Kang et al. 2010). Its sensitive responses to global climatic change make the detection of global climate change observable at its early stage (X. Liu et al. 2009). Research about the consequences of global warming over the TP includes the analysis of significant environmental changes (Cheng and Wu 2007; J. Liu et al. 2009; Su and Shi 2002; Xu and Liu 2007) and the elevation dependency of surface air temperature variation (Liu and Chen 2000; X. Liu et al. 2009; Qin et al. 2009; Thompson et al. 2003; Yang et al. 2014; You et al. 2010). However, whether the globally observed warming hiatus between 2001 and 2014 has counterparts in the high mountainous TP and, if so, what the consequences/impact of the recent hiatus (from 2001 to the present) over the TP are, has to our knowledge not been evaluated, in particularly using remote sensing datasets.

Unlike using station and simulation data, employing remote sensing techniques to analyze surface air temperature changes in high mountainous regions is a relatively recent field of research. The remote sensing approach can overcome the problem of lack of observational data in particular in the western TP and also offer insights into the physical processes and forcing mechanisms related to the elevation dependency of climatic warming or the warming hiatus over the TP. Therefore, this work will help enhance our understanding of the characteristics of recent climatic warming hiatus and climate change over the TP. After introducing station-based and remote sensing–based surface air temperature datasets, methods of analysis are presented (section 2). Station-based (section 3a) and remote sensing–based (section 3b) warming trends of mean, seasonality, and variability are introduced before a comparison is analyzed (section 3c), followed by a concluding summary (section 4).

2. Data, methods of analysis, and geographical setting

Most TP warming investigations are performed using near-surface air and soil temperature measurements from China Meteorological Administration (CMA) meteorological stations (Qin et al. 2009; Yan and Liu 2014). However, the whole TP, especially the western regions and the regions above 4800 m, cannot be fully represented only by data from those stations. This is because the number of stations is quite limited compared to the wide area where they are not distributed uniformly, as they are concentrated more in the central and eastern regions and below 4800 m (Fig. 1). And usually meteorological stations are located near population centers and therefore do not represent all the environments in a regions, limiting the acquisition of accurate spatial information about climate (Stisen et al. 2007; Yao and Zhang 2013).

Therefore, three datasets are used, including monthly mean temperature from 86 CMA meteorological stations,

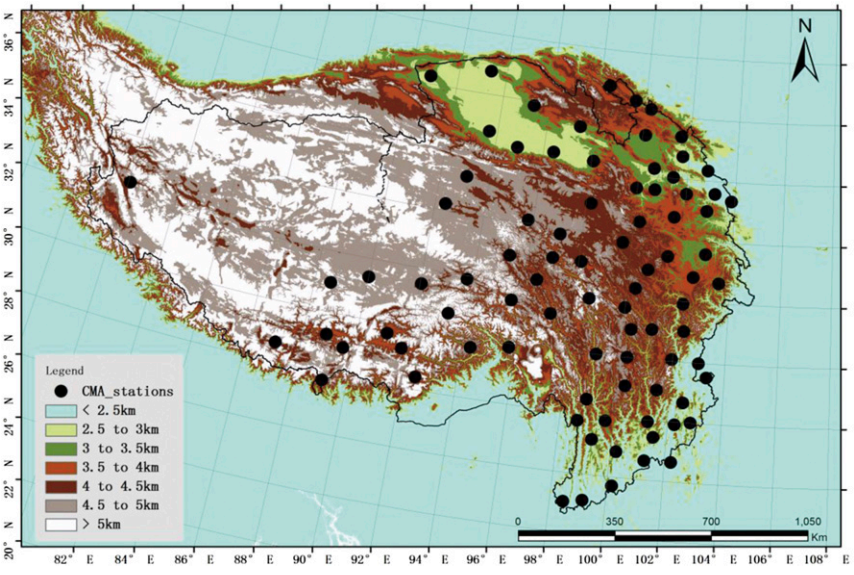

FIG. 1. Geographical setting of the Tibetan Plateau including digital elevation information (GTOPO30) and the location of 86 meteorological stations.

15 years of land surface temperature (LST) data from the Moderate Resolution Imaging Spectroradiometer (MODIS, MOD11C3, version 5), and the GTOPO30 global digital elevation model (DEM) from USGS. A period of 1961–2014 is selected from CMA data; detailed descriptions of data quality control and homogenization are available from Li et al. (2004). The MODIS LST data are monthly provided at 0.05° spatial resolution as a gridded level-3 product for daytime and nighttime from 2001 to 2015. To be comparable and to diagnose the two temperatures' altitudinal dependence, GTOPO30 DEM data are resampled according to the spatial resolution of MODIS LST data and the surface elevations of the 86 stations are extracted accordingly.

Intra-annual seasonality, mean, and degree-days are calculated before a simple linear regression model is used for obtaining the warming trend. Interannual warming trends of spring [March–May (MAM)], summer [June–August (JJA)], autumn [September–November (SON)], and winter [December–February (DJF)], annual mean, and degree-days of the surface air temperature are evaluated by an F test considering P values less than 0.05. Degree-days, which are commonly defined as the accumulated daily mean temperature exceeding the base temperature, are one of the most important indicators of climate changes (You et al. 2014). Base temperature is the lowest temperature at which metabolic processes result in a net substance gain in aboveground biomass (Sitte et al. 1999). Some research further differentiates base temperatures related to various plants such as wheat, sunflower, and corn relying on rough estimates (as presented in textbooks; see Aufammer 1998; Keller et al. 1997). In this study, a base of 0°C is chosen to calculate the accumulation and number of degree-days (ADD and NDD, respectively) characterizing annual biomass increase in the TP as well as interactions between the cryosphere, atmosphere, hydrosphere, ecosystem, and topographic complexity (Bengtsson 1976). Monthly mean temperature of meteorological station data and both daytime and nighttime monthly MODIS LST composites are included as surface temperature inputs. Surface temperature data (DD) serves here as a surrogate for available photosynthetically active radiation (De Beurs and Henebry 2004), which captures information of plant growth, biodiversity, and potential evapotranspiration (Bengtsson 1976; You et al. 2014). The function can be estimated or measured as follows:

If $\mathrm{DD}_i > 0$, then

$$\mathrm{ADD}_i = \mathrm{ADD}_{i-1} + \mathrm{DD}_i; \quad \mathrm{NDD}_i = \mathrm{NDD}_{i-1} + 1;$$

otherwise,

$$\mathrm{ADD}_i = \mathrm{ADD}_{i-1}; \quad \mathrm{NDD}_i = \mathrm{NDD}_{i-1},$$

where DD_i is the monthly increment of growing degree-days at month i and ADD_i (NDD_i) is the growing degree-days (number of degree-days) accumulated from January, $i \in \{1, 2, \ldots 12\}$. Finally, the averaged accumulated degree-days (AADD) are calculated as

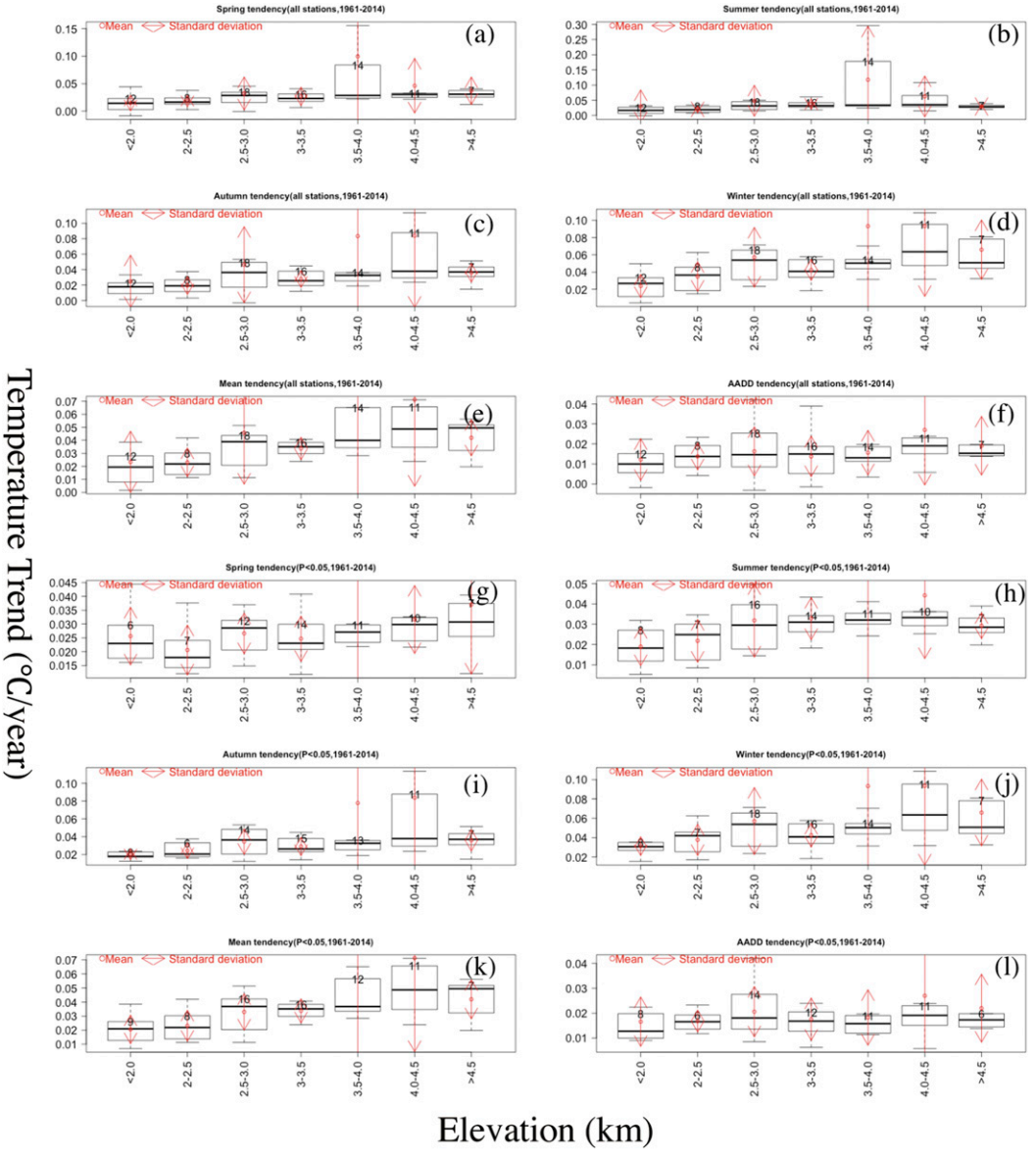

FIG. 2. Elevation-dependent warming trend statistics (0.5-km intervals, 1961–2014) at all meteorological stations and significant stations of statistical significance on 95% level with P values < 0.05: (a),(h) spring, (b),(i) summer, (c),(j) autumn, (d),(k) winter, (e),(l) mean, and (f),(m) averaged accumulative degree days (AADD). The number of stations is indicated in each box; missing boxes or fewer values mean that no or fewer stations pass the statistically significant F test.

$$\mathrm{AADD} = \sum_{1}^{12} \mathrm{ADD}_i \Big/ \sum_{1}^{12} \mathrm{NDD}_i .$$

3. Spatiotemporal temperature variability over the Tibetan Plateau

Analyzing climatic trends in mountainous and highland regions can be an ideal approach to the study of global warming hiatus due to their sensitivity and vulnerability to climate change (Messerli and Ives 1997). Elevation-dependent warming has been observed in several mountainous regions (Fyfe and Flato 1999; Giorgi et al. 1997; Pepin et al. 2015) besides the TP (X. Liu et al. 2009; Qin et al. 2009). To understand whether the recent slowdown in global warming occurs over the TP and, if that is the case, whether the elevation dependency of warming could

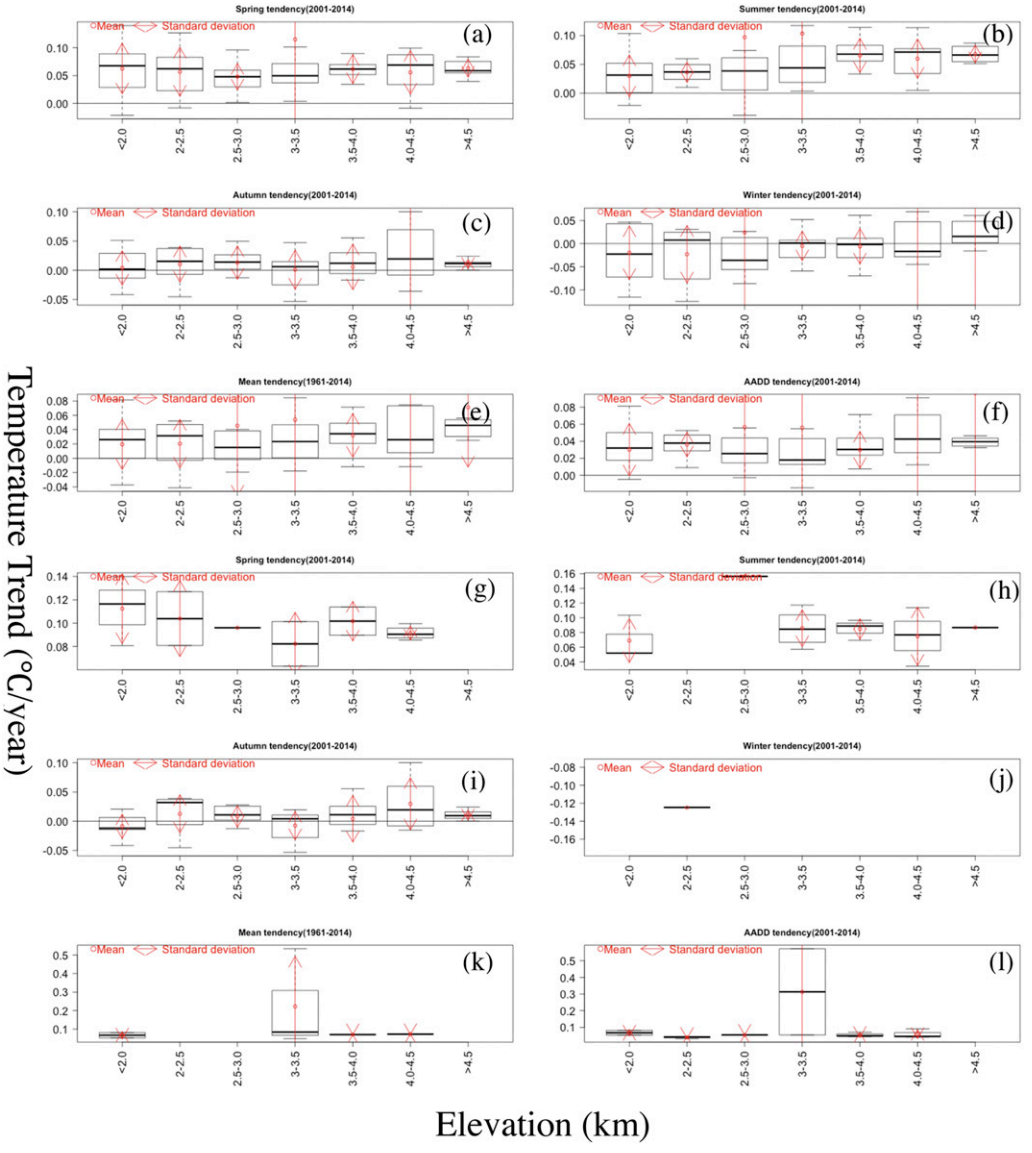

FIG. 3. As in Fig. 2, but for 2001–14.

still be observed, both meteorological stations and remote sensing–based warming trends are analyzed and compared.

a. Station-based warming trends

Warming trend analyses of the temperature time series from the 86 meteorological stations in the period of 1961–2014 are presented first displaying the long-term warming trend and its altitudinal dependency (Fig. 2). 1) Almost all the stations (or stations with statistically significant trends, 95% level) over the TP have experienced a notable warming during the last 54 years, with warming rates of 0.5° ± 0.73°C decade^{-1} (or 0.47° ± 0.73°C decade^{-1}) for the annual mean. 2) The seasonal warming rates of all the stations show linear warming rates of winter (0.59° ± 0.68°C decade^{-1}) > summer (0.53° ± 0.85°C decade^{-1}) > autumn (0.47° ± 0.77°C decade^{-1}) > spring (0.41° ± 0.76°C decade^{-1}), while the seasonal warming rates of stations with statistically significance show linear warming rates of winter (0.62° ± 0.69°C decade^{-1}) > autumn (0.46° ± 0.77°C decade^{-1}) > summer (0.40° ± 0.75°C decade^{-1}) > spring (0.37° ± 0.77°C decade^{-1}). That is, the most obvious warming occurs in winter, which is comparable with previous results given by X. Liu et al. (2009). 3) The linear warming rate of the averaged accumulated degree-days AADD for all stations (or stations with statistically significance) is 0.16° ± 0.14°C decade^{-1} (or

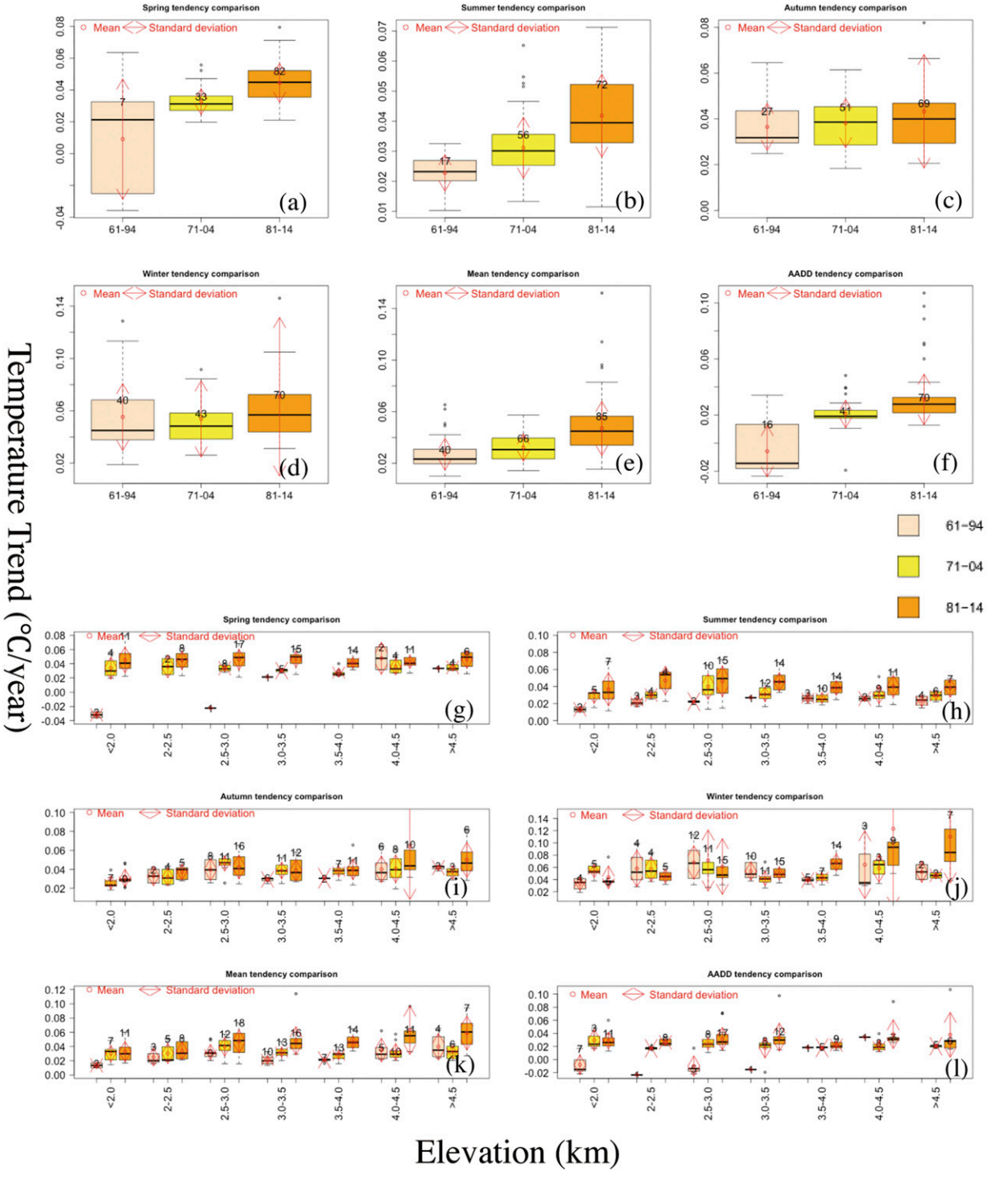

FIG. 4. As in Fig. 2, but comparing three periods (1961–94 vs 1971–2004 vs 1981–2014).

0.20° ± 0.14°C decade^{-1}), which may correspond with the greenness/vegetation increasing over the TP (Cai et al. 2015). 4) The linear trends (analyzed in 0.5-km elevation interval zones) show a positive altitudinal dependency, including annual mean, seasonality, and averaged accumulated degree-days. That is, the warming trends (during 1961–2014) increasing with elevation depend on seasonality.

TABLE 1. Elevation-dependent mean and standard deviation comparison (0.5-km intervals, 1961–94 vs 1971–2004 vs 1981–2014) of warming trends at meteorological stations with statistically significant trends (95% level, P value < 0.05) for spring, summer, autumn, winter, mean, and averaged accumulative degree days (AADD). NaN means that either no stations pass or only one station passes the statistically significant F test.

Mean (std) °C decade^{-1}		<2.0 km	2–2.5 km	2.5–3 km	3–3.5 km	3.5–4 km	4–4.5 km	>4.5 km
1961–94	Spring	−0.32 (0.06)	NaN	−0.22 (NaN)	0.21 (NaN)	NaN	0.48 (NaN)	0.33 (NaN)
	Summer	0.13 (0.04)	0.22 (0.07)	0.22 (0.01)	0.27 (NaN)	0.26 (0.06)	0.26 (0.04)	0.23 (0.07)
	Autumn	NaN	0.33 (0.10)	0.40 (0.12)	0.29 (0.02)	0.30 (0.00)	0.40 (0.14)	0.42 (0.03)
	Winter	0.33 (0.11)	0.58 (0.30)	0.68 (0.28)	0.54 (0.15)	0.39 (0.05)	0.64 (0.56)	0.52 (0.17)
	Mean	0.13 (0.05)	0.25 (0.13)	0.32 (0.11)	0.21 (0.06)	0.21 (0.03)	0.35 (0.17)	0.40 (0.19)
	AADD	−0.08 (0.15)	−0.24 (NaN)	−0.10 (NaN)	−0.15 (NaN)	0.18 (NaN)	0.34 (NaN)	NaN
1971–2004	Spring	0.34 (0.16)	0.36 (0.16)	0.34 (0.05)	0.30 (0.03)	0.28 (0.06)	0.36 (0.12)	0.35 (0.05)
	Summer	0.28 (0.08)	0.30 (0.04)	0.40 (0.15)	0.31 (0.09)	0.27 (0.06)	0.30 (0.11)	0.29 (0.05)
	Autumn	0.26 (0.07)	0.32 (0.09)	0.46 (0.08)	0.39 (0.09)	0.38 (0.06)	0.41 (0.15)	0.37 (0.07)
	Winter	0.54 (0.11)	0.57 (0.20)	0.71 (0.50)	0.42 (0.12)	0.43 (0.08)	0.58 (0.23)	0.47 (0.06)
	Mean	0.30 (0.12)	0.30 (0.14)	0.40 (0.13)	0.32 (0.07)	0.28 (0.07)	0.32 (0.12)	0.32 (0.09)
	AADD	0.30 (0.16)	0.17 (0.02)	0.25 (0.09)	0.18 (0.15)	0.18 (0.02)	0.21 (0.09)	0.20 (0.02)
1981–2014	Spring	0.45 (0.18)	0.45 (0.13)	0.46 (0.14)	0.46 (0.11)	0.41 (0.08)	0.43 (0.09)	0.46 (0.12)
	Summer	0.37 (0.19)	0.47 (0.17)	0.46 (0.18)	0.45 (0.11)	0.38 (0.09)	0.40 (0.13)	0.38 (0.11)
	Autumn	0.31 (0.09)	0.37 (0.08)	0.42 (0.13)	0.39 (0.11)	0.40 (0.11)	0.64 (0.56)	0.50 (0.19)
	Winter	0.44 (0.19)	0.46 (0.11)	0.61 (0.46)	0.50 (0.11)	0.68 (0.15)	1.23 (1.29)	1.10 (0.76)
	Mean	0.33 (0.15)	0.34 (0.13)	0.47 (0.16)	0.48 (0.20)	0.46 (0.09)	0.63 (0.34)	0.59 (0.24)
	AADD	0.29 (0.13)	0.26 (0.05)	0.32 (0.17)	0.34 (0.21)	0.22 (0.06)	0.39 (0.22)	0.38 (0.34)

Similar warming trend analyses for the 2001–14 interval are presented to investigate the possible discrepancies in the temperature trend and its altitude dependency between the 1961–2014 period and the recent hiatus (2001–present; see Fig. 3). 1) The recent analyses of all observational station data confirm the conclusions (see Fig. 2), which suggest that a pattern of warming has persisted up to 2014, with a linear warming rate of 0.48° ± 1.02°C decade^{-1} for the annual mean temperature and 0.66° ± 1.62°C decade^{-1} for the averaged accumulated degree-days. 2) A different seasonal order of linear warming rates shows summer (0.71° ± 1.51°C decade^{-1}) > spring (0.68° ± 1.16°C decade^{-1}) > winter (0.48° ± 1.02°C decade^{-1}) > autumn (0.33° ± 2.72°C decade^{-1}), with noticeable (remarkable) standard deviation values compared with similar statistics in the period of 1961–2014. 3) If only the last 14 years are considered, the trends are positive but insignificant (missing boxes or fewer values mean no or fewer stations satisfy the F test; see Figs. 3g–l). That is, for most of the stations, the recent warming trend may either be nonlinear or has come to a halt (without trend). The only exception is the autumn trend showing a statistically significant linear warming rate of 0.05° ± 0.30°C decade^{-1} (more statistically significant analyses will be shown in section 3b with remote sensing data). 4) The elevation dependency of climate warming is not as robust as it in the period of 1961–2014. For example, the statistically significant increasing rates of autumn temperature are −0.09° ± 0.21°, 0.13° ± 0.33°, 0.08° ± 0.18°, −0.08° ± 0.24°, 0.04° ± 0.40°, 0.30° ± 0.44°, and 0.11° ± 0.08°C decade^{-1} averaged for stations at <2 km, 2–2.5 km, 2.5–3 km, 3–3.5 km, 3.5–4 km, 4–4.5 km, and 4.5–5 km, respectively (Fig. 3i).

To further diagnose the recent warming trends and elevation dependency of temperature trends, three temperature trends are also analyzed and plotted in Fig. 4 and Table 1, showing the warming trend shift from 1961–94 to 1971–2004 to the most recent period 1981–2014 (all significance levels given in Fig. 4 are at the $P <$ 0.05 level). 1) Most of the stations over the TP have experienced statistically significant warming, particularly for the periods of 1971–2004 and 1981–2014. The warming rates increase as the periods shift (i.e., warming trend of 1961–94 < 1971–2004 < 1981–2014), which is independent from variable parameters, such as annual mean, seasonality, and averaged accumulated degree-days (Figs. 4a–f). 2) Significant station samples are not sufficiently representative in the period of 1961–94, as only winter and annual mean trends display complete "boxes" in all the elevation zones (Figs. 4g–l), showing positive elevation dependencies below and above ~3 km (likewise during 1971–2004). For example, the statistically significant increasing rates of annual mean (or winter) temperature in 1961–94 are 0.13° ± 0.05°C, 0.25 ± 0.13°C, and 0.32° ± 0.11°C decade^{-1}

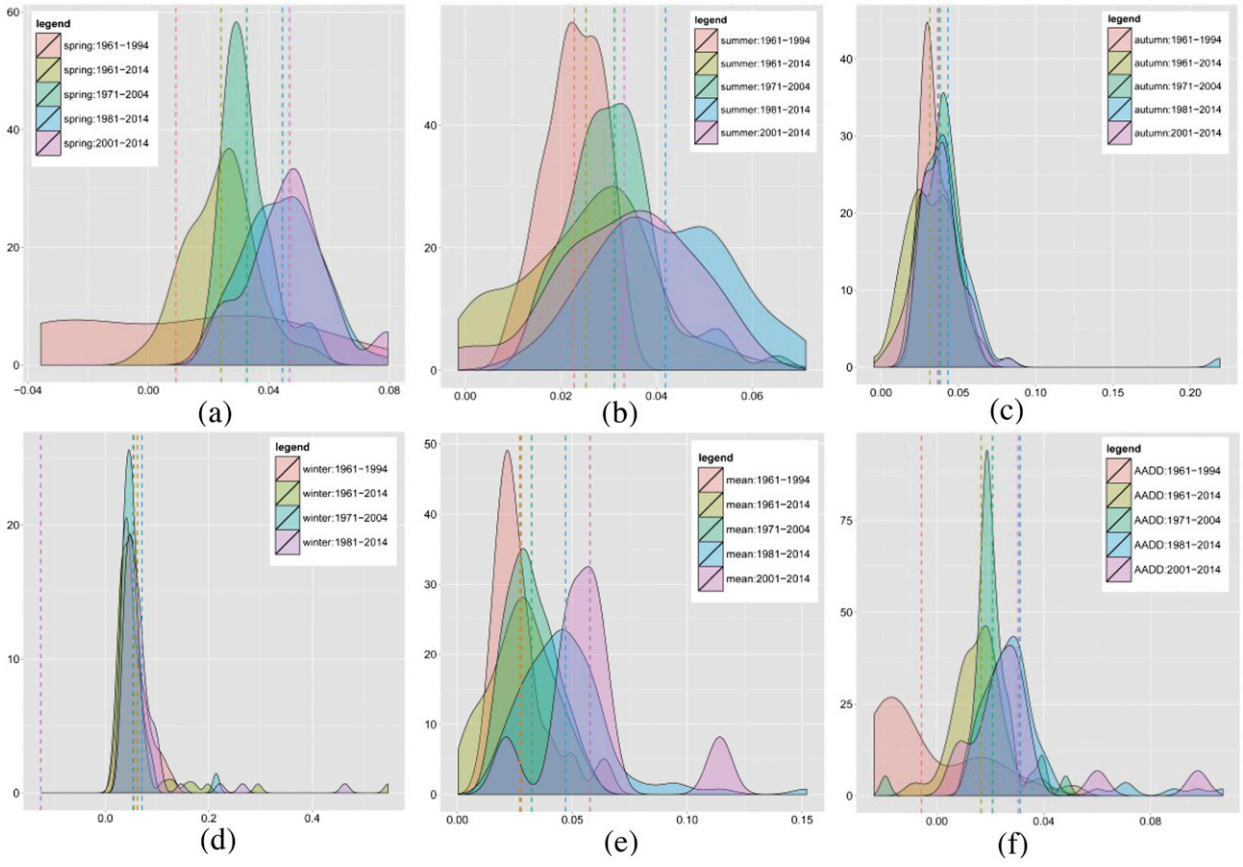

FIG. 5. Histograms (1961–94 vs 1971–2004 vs 1981–2014 vs 2001–14 vs 1961–2014) of warming trends using meteorological station data with statistically significant trends (95% level, P value < 0.05): (a) spring, (b) summer, (c) autumn, (d) winter, (e) mean, and (f) averaged accumulative degree days over the Tibetan Plateau. The number of stations is indicated in each box; missing boxes or fewer values mean no or less stations pass the statistically significant F test.

(or 0.33° ± 0.11°C, 0.58° ± 0.30°C, and 0.68° ± 0.28 °C decade^{-1}) averaged for stations at <2 km, 2–2.5 km, and 2.5–3 km, respectively. The threshold of ~3 km is also found by Qin et al. (2009). 3) During 1981–2014 the elevation-dependent temperature trends are most robust for winter means, followed by annual means and autumn seasons.

Histograms for the five different periods—1961–94, 1971–2004, 1981–2014, the most recent period 2001–14, and the whole period of 1961–2014—also confirm that there is no clear shift from predominant warming to near stagnation during the most recent periods. The warming trend over the TP has experienced a statistically significant continuous warming during the last 54 years that is independent of seasonality (see the histogram of warming rates in Fig. 5).

b. *Remote sensing–based warming trends*

Unlike previous studies considering warming rate from CMA stations and the one from MODIS LST data at station corresponding pixels (Qin et al. 2009), MODIS LST data are analyzed as an independent dataset to obtain temperature change trends. This is because statistically significant grid pixels in MODIS data appear to show a more representative distribution of the wide mountainous regions than meteorological station data (see Figs. 6 and 7 vs Fig. 1). Incomplete coverage of the observational statistically significant temperature data leads to a possible data bias of the warming rate estimation if only the last 14 years are considered (see missing ''boxes'' in Figs. 3g–l).

Related daytime and nighttime geographical distribution of temperature trends and P value from the F test are presented in Figs. 6 and 7, which show the following results: 1) Regression slopes along the Himalaya and Kunlun Mountains indicate a cooling trend (shown in green), especially in spring and winter as well as the annual means and averaged accumulated degree-days. 2) The warming trend occurs more frequently in the Hengduan Mountain Range where most of the meteorological stations are located. 3) A smoother and more robust warming trend distribution is noted for nighttime

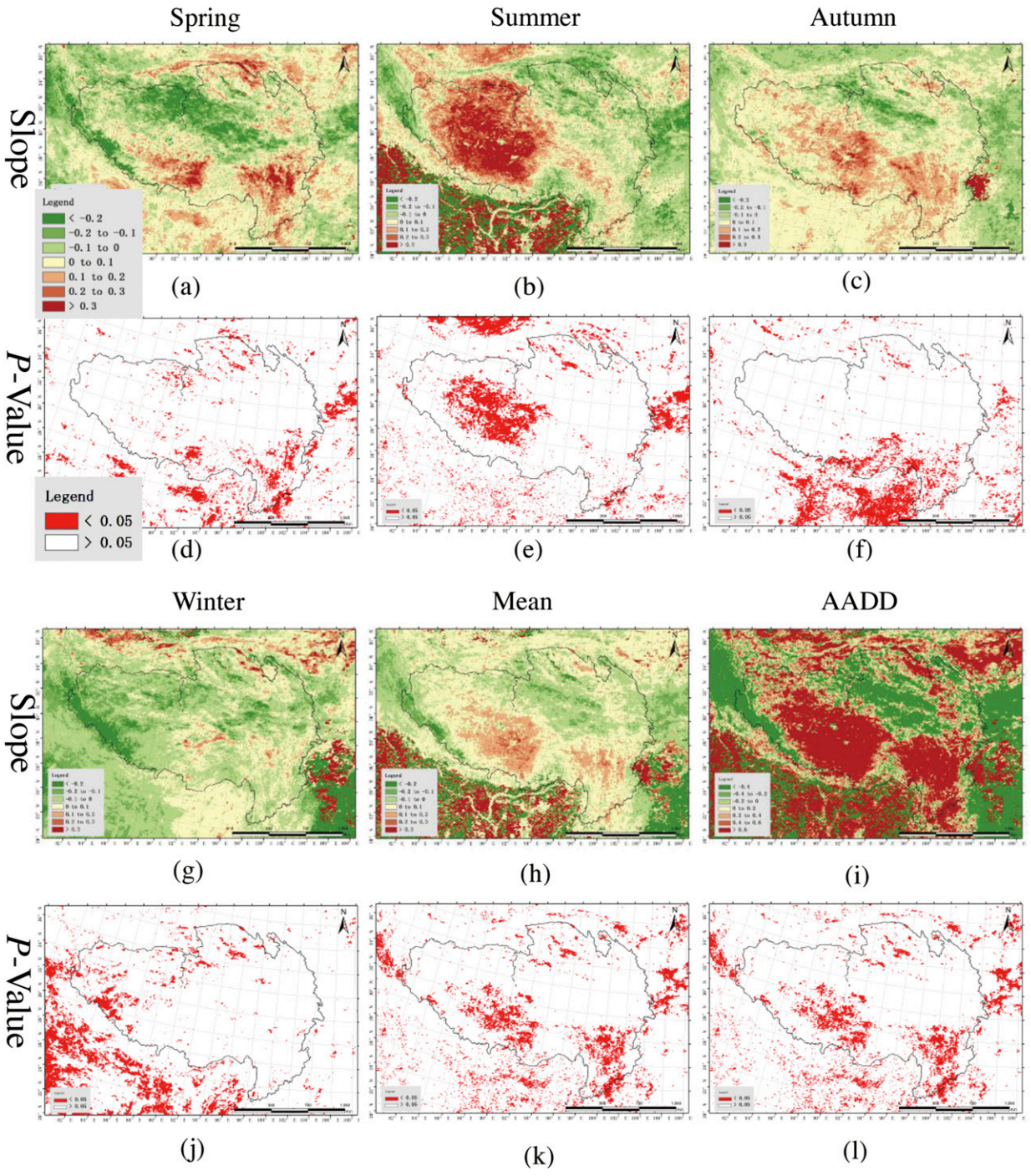

FIG. 6. Geographical distribution of MODIS daytime LST (2001–15) analysis for spring (MAM), summer (JJA), autumn (SON), winter (DJF), annual mean, and averaged accumulated degree-days (AADD)-based regression (a)–(c) and (g)–(i) trend and (d)–(f) and (j)–(l) *P* value.

compared with (also regionally varying) daytime LST trends.

Detailed statistical analyses with MODIS daytime and nighttime LSTs for the period of 2001–15 are shown in Figs. 8 and 9 to focus on the possible remote sensing–based temperature trends and altitudinal dependencies since the recent hiatus (2001 to the present). To clearly display remote sensing data against measurements, the

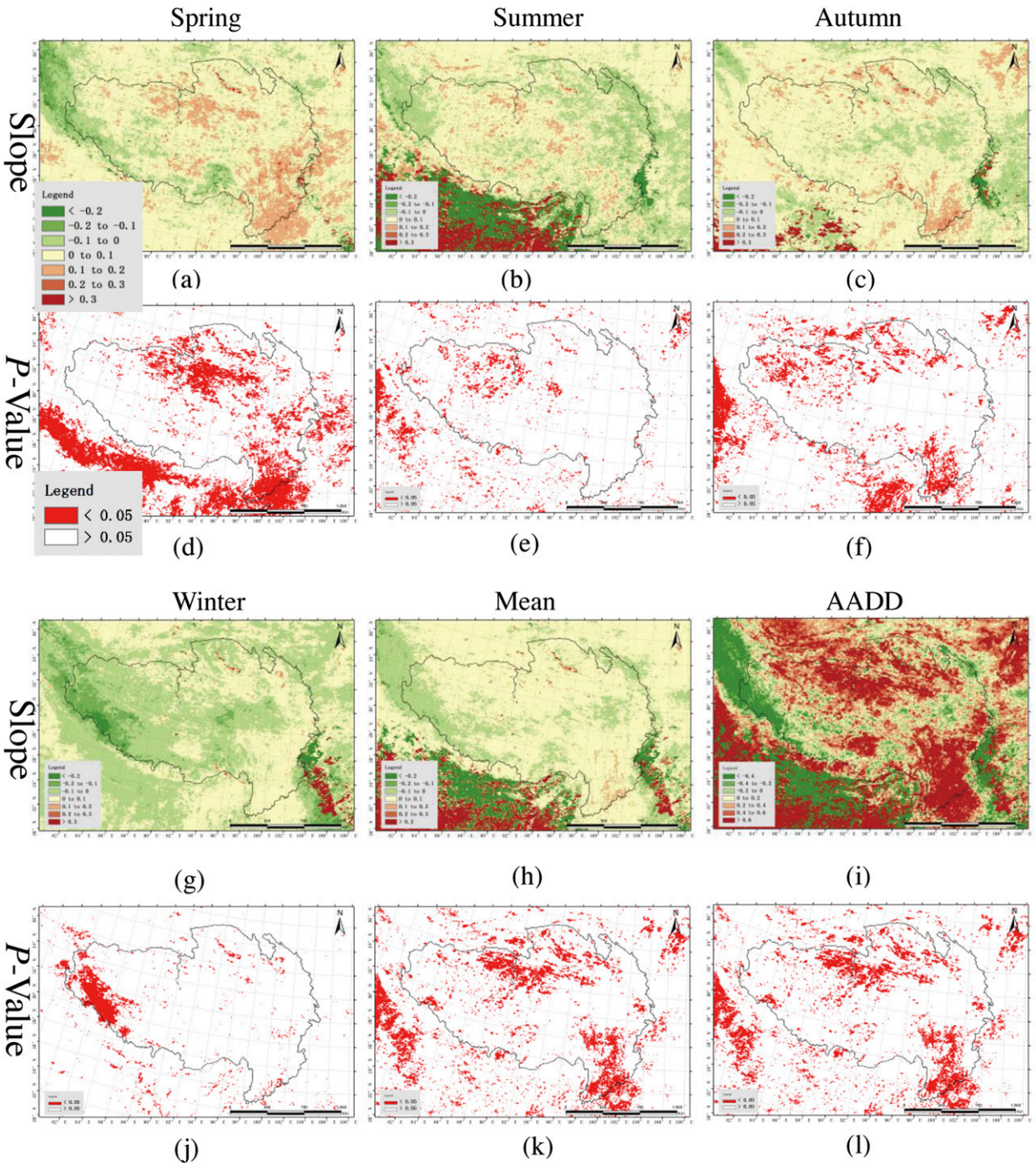

FIG. 7. As in Fig. 6, but for nighttime.

range above 2.0 km is chosen because a large pixel number (below 2.0 km) and high standard deviations do not reveal clear trends and altitude dependencies. The following results are noted. First, for the entire TP with elevation above 2 km (Figs. 8a–f and 9a–f), 63.33% (76.91%) of the pixels have experienced a notable warming during the most recent 15 years using LST daytime (nighttime) series with a linear warming rate of $0.27° \pm 0.86°C\,decade^{-1}$ ($0.25° \pm 0.39°C\,decade^{-1}$) for the annual mean. Contrarily, for the significant regions (P value < 0.05; Figs. 8g–l and 9g–l), 14.26% (18.29%) of the pixels have experienced a statistically significant

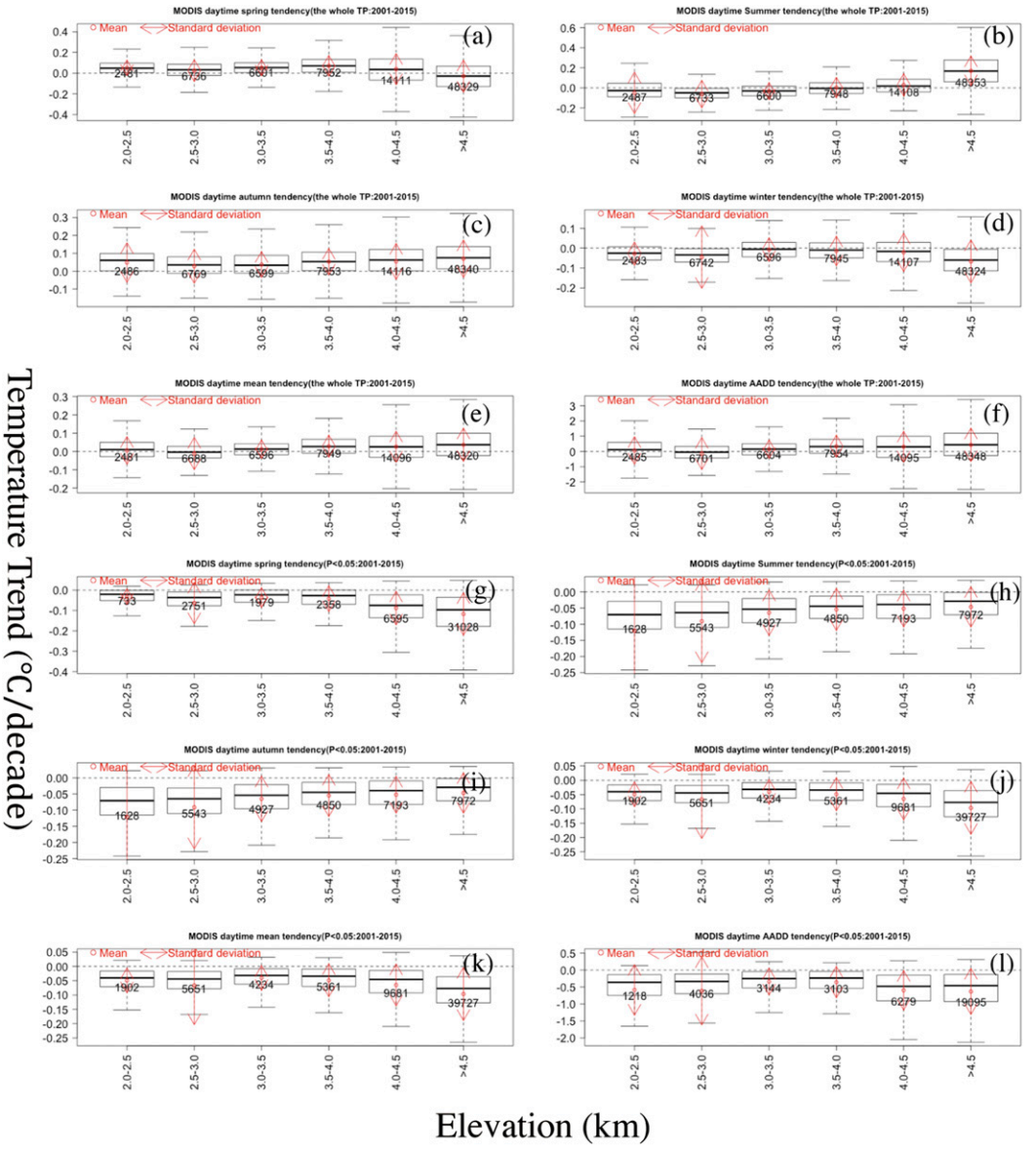

FIG. 8. Elevation-dependent warming trend statistics (0.5-km intervals, 2001–15) derived from MODIS daytime land surface temperature (LST) over the Tibetan Plateau and significant regions with warming trends passing the F test at the 95% level (P value < 0.05): (a),(h) spring, (b),(i) summer, (c),(j) autumn, (d),(k) winter, (e),(l) mean, and (f),(m) averaged accumulative degree days (AADD). Pixel number is indicated in each box, and missing boxes or fewer values mean no or less stations pass the statistically significant F test.

warming during the most recent 15 years with LST daytime (nighttime) series, showing a linear cooling rate of $-0.48° \pm 0.57°C\,decade^{-1}$ ($-0.18 \pm 0.25°C\,decade^{-1}$) for the annual mean.

Second, the seasonal trends over the entire TP show linear warming rates of daytime trends of summer ($0.92° \pm 1.64°C\,decade^{-1}$) > autumn ($0.60° \pm 1.0°C\,decade^{-1}$) > spring ($0.04° \pm 1.45°C\,decade^{-1}$) > winter ($-0.47° \pm 1.07°C\,decade^{-1}$), and nighttime trends of spring ($0.54° \pm 0.63°C\,decade^{-1}$) > autumn ($0.44° \pm 0.5°C\,decade^{-1}$) > summer ($0.25° \pm 0.58°C\,decade^{-1}$) > winter ($-0.21° \pm 0.69°C\,decade^{-1}$). However, the seasonal trends in statistically significant regions show linear cooling rates of daytime trends of autumn ($-0.52° \pm 0.72°C\,decade^{-1}$) > summer ($-0.63° \pm 0.93°C\,decade^{-1}$) > winter ($-0.81° \pm 0.91°C\,decade^{-1}$) > spring ($-1.0° \pm 1.0°C\,decade^{-1}$), and nighttime trends of autumn ($-0.19° \pm 0.27°C\,decade^{-1}$) > summer ($-0.30° \pm 0.33°C\,decade^{-1}$) > spring ($-0.32° \pm 0.40°C\,decade^{-1}$) > winter ($-0.51° \pm 0.60°C\,decade^{-1}$). Thus, the most obvious seasonal trend discrepancy

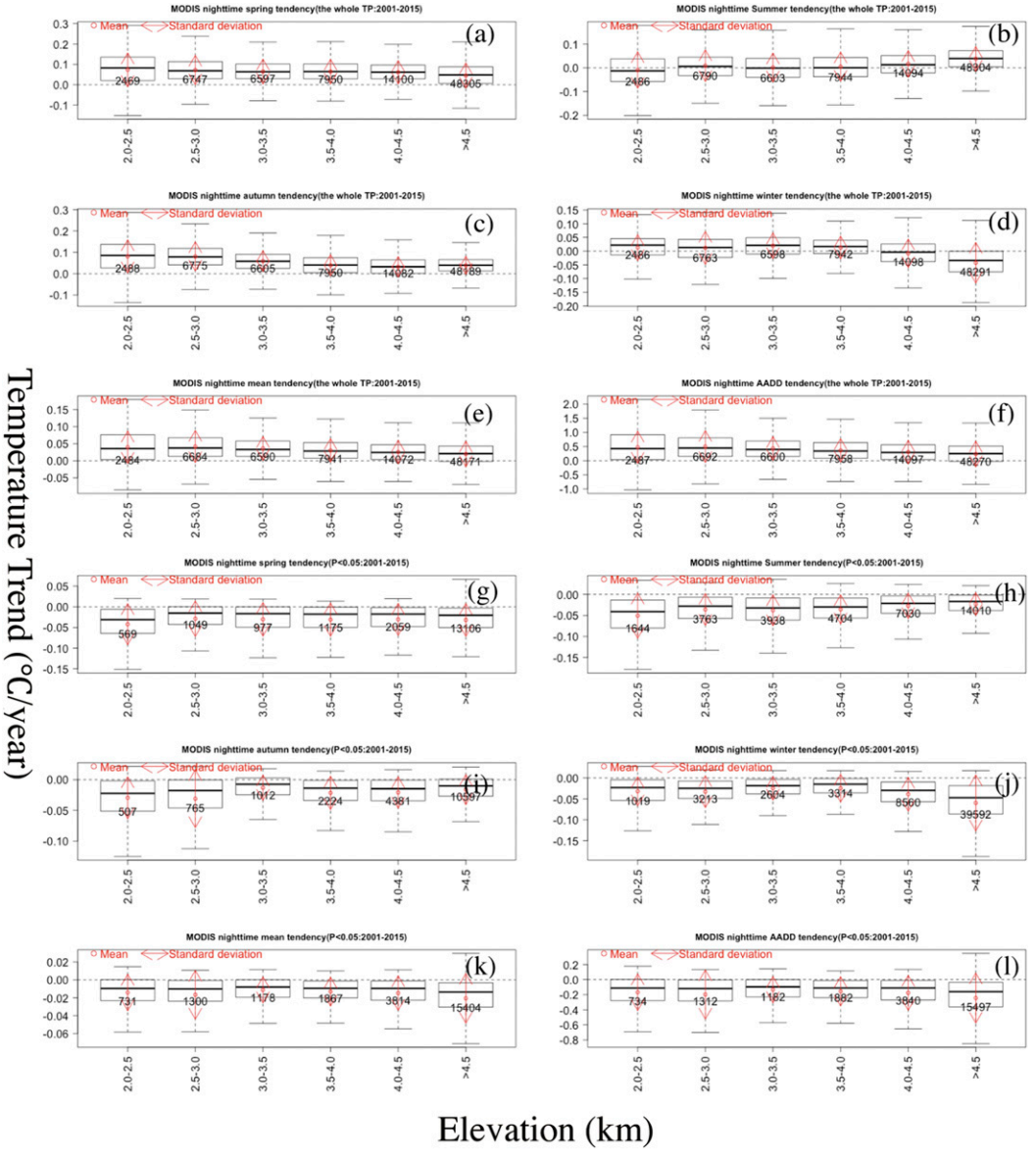

FIG. 9. As in Fig. 8, but for nighttime.

between averaged MODIS daytime and nighttime LSTs and meteorological station data occurs in winter. This discrepancy could be due to the limitations of remote sensing reflection data over surfaces with high albedo (ice and snow), because in mountainous areas with large terrain slopes a main radiative artifact is related to the angle dependence of satellite observations.

Third, the MODIS LST-based elevation dependencies show both positive or negative and robust or weak correlations depending on statistical parameters, such as annual mean, seasonality, and averaged accumulated degree-days, although similar elevation dependencies are indicated in significant regions and for the entire TP. For example, the statistically significant cooling rates of the daytime spring trends show a negative elevation dependency versus daytime summer trends showing a positive elevation dependency. This finding is comparable with previous results (Vuille and Bradley 2000; Pepin and Seidel 2005; Pepin and Lundquist 2008; You et al. 2010) that elevation dependency could not be confirmed in various regions of the world.

c. *Elevation dependence: A comparison*

To compare elevation dependencies of CMA stations and MODIS LST data, temperature trends from CMA

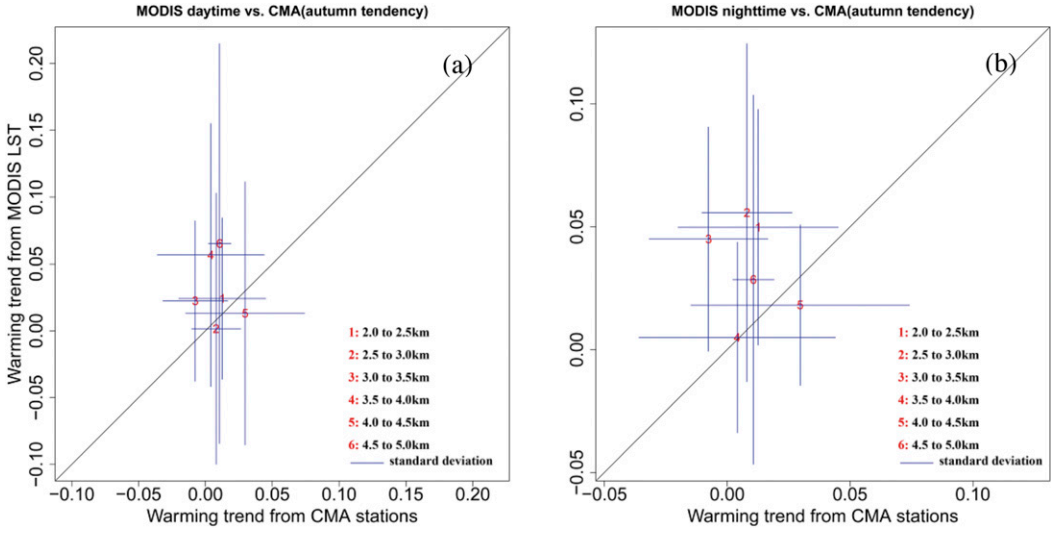

FIG. 10. Comparison between warming trends derived from station observations (with a statistically significance at the 95% level) and from station-related MODIS pixels: (a) daytime and (b) nighttime LST trends with an elevation interval of 0.5 km. For station observations only the autumn trend shows sufficient significance in all elevation zones.

stations are selected exceeding the statistically significance of 95% (P value < 0.05). That is, only autumn trends from CMA station data passing the F test (for 2001–14, see Figs. 3g,h) will be compared with MODIS daytime and nighttime LST data (Fig. 10). 1) Similar autumn trends from MODIS daytime and nighttime LST data are extracted at station corresponding pixels. Warming trends from the related remotely sensed MODIS spectroradiometer data are relatively more intense than observed by the 86 meteorological stations. They show higher mean values in most of the elevations zones and more variability (standard deviation) of daytime (compared to nighttime) trends. Thus, it may be possible that there is a positive bias in the remotely sensed MODIS warming trends. 2) The statistically significant MODIS temperature trends (Figs. 8g–l and 9g–l) show a cooling trend in the significant regions instead of warming. Although the entire TP indicates a warming trend (Figs. 8a–f and 9a–f), regional cooling is missing when considering only the CMA station data. 3) In summarizing, the general warming rate derived merely from the limited number of samples/stations may not be fully representative for the warming status of the entire TP. That is, studies based only on station observations do not necessarily provide a representative and complete picture of temperature change estimates observed over the TP. But it needs to be noted that the general updated and detailed warming distribution obtained from MODIS LST data [warming dependences on complex topography, time phases (seasonal, diurnal, and nocturnal) and altitude] are based on the assumption that in regions without station measurements, MODIS LST data provide trends similar to those from station-based temperature observations (see also Qin et al. 2009).

4. Summary and conclusions

Fully quantifying the temperature change over the TP has profound implications for detecting early signals of global warming change (X. Liu et al. 2009) and for better understanding the influence of the TP on its surrounding regions in terms of water cycle, atmospheric circulation, and environment change (Yao et al. 2004). The aim of this study is to provide a clearer picture of the magnitude, change, and spatiotemporal characteristics of surface air temperature changes over the TP using both station network and remote sensing observations. This includes the elevation dependency of warming and the recent globally observed slowdown and whether it occurs over the TP.

Analyses applied to the geographically and climatically complex TP shows the following results:

1) The entire TP indicates a warming trend from 1961 to 2014, and no cooling shift is found from the predominant warming from 1961–94 and 1971–2004 to the most recent periods of 1981–2014 and 2001–14 using meteorological station data.
2) The MODIS daytime and nighttime LST trends derived from station corresponding pixels show a higher mean value in most of the elevations zones, but a lower warming trend for the entire TP of $0.27° \pm 0.86°C\,decade^{-1}$ or $0.25° \pm 0.39°C\,decade^{-1}$,

and even a cooling trend for the significant regions of $-0.48° \pm 0.57°C\,decade^{-1}$ or $-0.18° \pm 0.25°C\,decade^{-1}$ in terms of daytime or nighttime mean trend. That is, the warming rate derived from limited CMA observations is not representative.

3) The analysis of the TP temperature trends shows continuing warming for higher elevations and a positive warming–elevation correlation from 1961 to 2014. However, the positive warming–elevation correlation could not be confirmed for different periods and regional scales. That is, distinct differences in terms of stagnant temperatures or even cooling have been observed in different periods and regions.
4) Recent analyses suggest (Dai et al. 2015; Steinman et al. 2015; Watanabe et al. 2014) that the global warming hiatus is mainly induced by internal natural decadal climate variations originating from the Pacific and Atlantic that lead to regionally varying responses on land temperature and precipitation (Dai 2013; Dai et al. 2015). Thus the response of the Tibetan Plateau (or any other regions) may be affected by signals that are transported by the dynamics of large-scale atmospheric circulation (see Zhu et al. 2011). The statistics of this response, however, is subject to further analyses, in particular the relevance of the temperature trends.

In general, although remote sensing data may partially contradict the warming trends observed in the station data, as it occurs mainly in regions of central TP that are sparsely covered by ground-based measurements, this study shows that the globally observed warming hiatus between 2001 and 2014 has no counterparts in the high mountainous TP. In particular, the station data suggest that the warming is almost continuously ongoing in the time interval 1961–2014. That is, the TP has experienced a statistically significant warming during the last 54 years and no distinct hiatus could be found in the last 15 years. In addition, previous studies based on station observations do not provide the complete picture for the temperature change over the TP. Regional, seasonal, and altitudinal differences make warming trend analyses complex, so warming trends can easily be underestimated or neglected. Here, remote sensing–based LST datasets have the potential to identify early signals of regional climate changes that can be used in assessing the environmental impacts of global climate changes in mountainous regions. Further research will focus on the impacts of multispheric and multiscale interactions on climate changes, in particular the interrelationship between the cryosphere in terms of snow cover (albedo), vegetation, and enlarged lake areas and the seasonal, diurnal, and altitudinal discrepancies over the TP.

Acknowledgments. Support by the Chinese National Science Foundation (Grant 41501375), by the Key Laboratory of Meteorological Disaster of Ministry of Education, Nanjing University of Information Science and Technology (Grant KLME1510), and by the Max Planck Fellow Group (DC, KF) is acknowledged.

REFERENCES

Amaya, D. J., S.-P. Xie, A. J. Miller, and M. J. McPhaden, 2015: Seasonality of tropical Pacific decadal trends associated with the 21st century global warming hiatus. *J. Geophys. Res. Oceans*, **120**, 6782–6798, doi:10.1002/2015JC010906.

Aufammer, W., 1998: *Getreide- und andere Körnerfruchtarten: Bedeutung, Nutzung und Anbau*. Eugen Ulmer, 560 pp.

Bengtsson, L., 1976: Snowmelt estimated from energy budget studies. *Hydrol. Res.*, **7**, 3–18.

Cai, D., Y. Guan, S. Guo, C. Zhang, and K. Fraedrich, 2014: Mapping plant functional types over broad mountainous regions: A hierarchical soft time-space classification applied to the Tibetan Plateau. *Remote Sens.*, **6**, 3511–3532, doi:10.3390/rs6043511.

——, K. Fraedrich, F. Sielmann, L. Zhang, X. Zhu, S. Guo, and Y. Guan, 2015: Vegetation dynamics on the Tibetan Plateau (1982–2006): An attribution by ecohydrological diagnostics. *J. Climate*, **28**, 4576–4584, doi:10.1175/JCLI-D-14-00692.1.

Chen, Y., Z. Li, Y. Fan, H. Wang, and H. Deng, 2015: Progress and prospects of climate change impacts on hydrology in the arid region of northwest China. *Environ. Res.*, **139**, 11–19, doi:10.1016/j.envres.2014.12.029.

Cheng, G., and T. Wu, 2007: Responses of permafrost to climate change and their environmental significance, Qinghai-Tibet Plateau. *J. Geophys. Res.*, **112**, F02S03, doi:10.1029/2006JF000631.

Cowtan, K., and R. G. Way, 2014: Coverage bias in the HadCRUT4 temperature series and its impact on recent temperature trends. *Quart. J. Roy. Meteor. Soc.*, **140**, 1935–1944, doi:10.1002/qj.2297.

Dai, A., 2013: The influence of the inter-decadal Pacific oscillation on US precipitation during 1923–2010. *Climate Dyn.*, **41**, 633–646, doi:10.1007/s00382-012-1446-5.

——, J. C. Fyfe, S.-P. Xie, and X. Dai, 2015: Decadal modulation of global surface temperature by internal climate variability. *Nat. Climate Change*, **5**, 555–559, doi:10.1038/nclimate2605.

De Beurs, K. M., and G. M. Henebry, 2004: Land surface phenology, climatic variation, and institutional change: Analyzing agricultural land cover change in Kazakhstan. *Remote Sens. Environ.*, **89**, 497–509, doi:10.1016/j.rse.2003.11.006.

Delworth, T. L., F. R. Zeng, A. Rosati, G. A. Vecchi, and A. T. Wittenberg, 2015: A link between the hiatus in global warming and North American drought. *J. Climate*, **28**, 3834–3845, doi:10.1175/JCLI-D-14-00616.1.

Dong, B., and A. Dai, 2015: The influence of the interdecadal Pacific oscillation on temperature and precipitation over the globe. *Climate Dyn.*, **45**, 2667–2681, doi:10.1007/s00382-015-2500-x.

Easterling, D. R., and M. F. Wehner, 2009: Is the climate warming or cooling? *Geophys. Res. Lett.*, **36**, L08706, doi:10.1029/2009GL037810.

England, M. H., and Coauthors, 2014: Recent intensification of wind-driven circulation in the Pacific and the ongoing warming hiatus. *Nat. Climate Change*, **4**, 222–227, doi:10.1038/nclimate2106.

Foster, G., and S. Rahmstorf, 2011: Global temperature evolution 1979–2010. *Environ. Res. Lett.*, **6**, 044022, doi:10.1088/1748-9326/6/4/044022.

Fyfe, J. C., and G. M. Flato, 1999: Enhanced climate change and its detection over the Rocky Mountains. *J. Climate*, **12**, 230–243, doi:10.1175/1520-0442-12.1.230.

——, N. P. Gillett, and F. W. Zwiers, 2013: Overestimated global warming over the past 20 years. *Nat. Climate Change*, **3**, 767–769, doi:10.1038/nclimate1972.

Giorgi, F., J. W. Hurrell, M. R. Marinucci, and M. Beniston, 1997: Elevation dependency of the surface climate change signal: A model study. *J. Climate*, **10**, 288–296, doi:10.1175/1520-0442(1997)010<0288:EDOTSC>2.0.CO;2.

Gleisner, H., P. Thejll, B. Christiansen, and J. K. Nielsen, 2015: Recent global warming hiatus dominated by low-latitude temperature trends in surface and troposphere data. *Geophys. Res. Lett.*, **42**, 510–517, doi:10.1002/2014GL062596.

Guemas, V., F. J. Doblas-Reyes, I. Andreu-Burillo, and M. Asif, 2013: Retrospective prediction of the global warming slowdown in the past decade. *Nat. Climate Change*, **3**, 649–653, doi:10.1038/nclimate1863.

Hansen, J., M. Sato, P. Kharecha, and K. von Schuckmann, 2011: Earth's energy imbalance and implications. *Atmos. Chem. Phys.*, **11**, 13 421–13 449, doi:10.5194/acp-11-13421-2011.

Hartmann, D., and Coauthors, 2013: Observations: Atmosphere and surface. *Climate Change 2013: The Physical Science Basis*, T. F. Stocker et al., Eds., Cambridge University Press, 159–254.

Kang, S., Y. Xu, Q. You, W.-A. Flügel, N. Pepin, and T. Yao, 2010: Review of climate and cryospheric change in the Tibetan Plateau. *Environ. Res. Lett.*, **5**, 015101, doi:10.1088/1748-9326/5/1/015101.

Karl, T. R., and Coauthors, 2015: Possible artifacts of data biases in the recent global surface warming hiatus. *Science*, **348**, 1469–1472, doi:10.1126/science.aaa5632.

Keller, E., H. Hanus, and K.-U. Heyland, 1997: *Grundlagen der landwirtschaftlichen Pflanzenproduktion.* Eugen Ulmer, 860 pp.

Kosaka, Y., and S.-P. Xie, 2013: Recent global-warming hiatus tied to equatorial Pacific surface cooling. *Nature*, **501**, 403–407, doi:10.1038/nature12534.

Li, Q., X. Liu, H. Zhang, T. C. Peterson, and D. R. Easterling, 2004: Detecting and adjusting temporal inhomogeneity in Chinese mean surface air temperature data. *Adv. Atmos. Sci.*, **21**, 260–268, doi:10.1007/BF02915712.

Liu, J., S. Wang, S. Yu, D. Yang, and L. Zhang, 2009: Climate warming and growth of high-elevation inland lakes on the Tibetan Plateau. *Global Planet. Change*, **67**, 209–217, doi:10.1016/j.gloplacha.2009.03.010.

Liu, X., and B. Chen, 2000: Climatic warming in the Tibetan Plateau during recent decades. *Int. J. Climatol.*, **20**, 1729–1742, doi:10.1002/1097-0088(20001130)20:14<1729::AID-JOC556>3.0.CO;2-Y.

——, Z. Cheng, L. Yan, and Z.-Y. Yin, 2009: Elevation dependency of recent and future minimum surface air temperature trends in the Tibetan Plateau and its surroundings. *Global Planet. Change*, **68**, 164–174, doi:10.1016/j.gloplacha.2009.03.017.

Meehl, G. A., J. M. Arblaster, J. T. Fasullo, A. Hu, and K. E. Trenberth, 2011: Model-based evidence of deep-ocean heat uptake during surface-temperature hiatus periods. *Nat. Climate Change*, **1**, 360–364, doi:10.1038/nclimate1229.

——, H. Teng, and J. M. Arblaster, 2014: Climate model simulations of the observed early-2000s hiatus of global warming. *Nat. Climate Change*, **4**, 898–902, doi:10.1038/nclimate2357.

Messerli, B., and J. D. Ives, 1997: *Mountains of the World: A Global Priority*. Parthenon, 510 pp.

Otto, A., and Coauthors, 2013: Energy budget constraints on climate response. *Nat. Geosci.*, **6**, 415–416, doi:10.1038/ngeo1836.

Pepin, N., and D. J. Seidel, 2005: A global comparison of surface and free-air temperatures at high elevations. *J. Geophys. Res.*, **110**, D03104, doi:10.1029/2004JD005047.

——, and J. Lundquist, 2008: Temperature trends at high elevations: Patterns across the globe. *Geophys. Res. Lett.*, **35**, L14701, doi:10.1029/2008GL034026.

——, and Coauthors, 2015: Elevation-dependent warming in mountain regions of the world. *Nat. Climate Change*, **5**, 424–430, doi:10.1038/nclimate2563.

Qin, J., K. Yang, S. Liang, and X. Guo, 2009: The altitudinal dependence of recent rapid warming over the Tibetan Plateau. *Climatic Change*, **97**, 321–327, doi:10.1007/s10584-009-9733-9.

Rabatel, A., and Coauthors, 2013: Current state of glaciers in the tropical Andes: A multi-century perspective on glacier evolution and climate change. *Cryosphere*, **7**, 81–102, doi:10.5194/tc-7-81-2013.

Santer, B. D., and Coauthors, 2014: Volcanic contribution to decadal changes in tropospheric temperature. *Nat. Geosci.*, **7**, 185–189, doi:10.1038/ngeo2098.

Schauwecker, S., and Coauthors, 2014: Climate trends and glacier retreat in the Cordillera Blanca, Peru, revisited. *Global Planet. Change*, **119**, 85–97, doi:10.1016/j.gloplacha.2014.05.005.

Schmidt, G. A., D. T. Shindell, and K. Tsigaridis, 2014: Reconciling warming trends. *Nat. Geosci.*, **7**, 158–160, doi:10.1038/ngeo2105.

Sitte, P., H. Ziegler, F. Ehrendorfer, and A. Bresinsky, 1999: *Lehrbuch der Botanik*, 34th ed. Fischer, 1176 pp.

Steinman, B. A., M. E. Mann, and S. K. Miller, 2015: Atlantic and Pacific multidecadal oscillations and Northern Hemisphere temperatures. *Science*, **347**, 988–991, doi:10.1126/science.1257856.

Stisen, S., I. Sandholt, A. Nørgaard, R. Fensholt, and L. Eklundh, 2007: Estimation of diurnal air temperature using MSG SEVIRI data in West Africa. *Remote Sens. Environ.*, **110**, 262–274, doi:10.1016/j.rse.2007.02.025.

Su, Z., and Y. Shi, 2002: Response of monsoonal temperate glaciers to global warming since the Little Ice Age. *Quat. Int.*, **97–98**, 123–131, doi:10.1016/S1040-6182(02)00057-5.

Thompson, L. G., E. Mosley-Thompson, M. E. Davis, P.-N. Lin, K. Henderson, and T. A. Mashiotta, 2003: Tropical glacier and ice core evidence of climate change on annual to millennial time scales. *Climate Variability and Change in High Elevation Regions: Past, Present & Future*, H. F. Diaz, Ed., Springer, 137–155.

Tollefson, J., 2014: Climate change: The case of the missing heat. *Nature*, **505**, 276–278, doi:10.1038/505276a.

Trenberth, K. E., and J. T. Fasullo, 2013: An apparent hiatus in global warming? *Earth's Future*, **1**, 19–32, doi:10.1002/2013EF000165.

Vuille, M., and R. S. Bradley, 2000: Mean annual temperature trends and their vertical structure in the tropical Andes. *Geophys. Res. Lett.*, **27**, 3885–3888, doi:10.1029/2000GL011871.

——, E. Franquist, R. Garreaud, L. Casimiro, W. Sven, and B. Cáceres, 2015: Impact of the global warming hiatus on Andean temperature. *J. Geophys. Res. Atmos.*, **120**, 3745–3757, doi:10.1002/2015JD023126.

Watanabe, M., H. Shiogama, H. Tatebe, M. Hayashi, M. Ishii, and M. Kimoto, 2014: Contribution of natural decadal variability to global warming acceleration and hiatus. *Nat. Climate Change*, **4**, 893–897, doi:10.1038/nclimate2355.

Xu, W., and X. Liu, 2007: Response of vegetation in the Qinghai-Tibet Plateau to global warming. *Chin. Geogr. Sci.*, **17**, 151–159, doi:10.1007/s11769-007-0151-5.

Yan, L., and X. Liu, 2014: Has climatic warming over the Tibetan Plateau paused or continued in recent years? *J. Earth Ocean Atmos. Sci.*, **1**, 13–28.

Yang, K., H. Wu, J. Qin, C. Lin, W. Tang, and Y. Chen, 2014: Recent climate changes over the Tibetan Plateau and their impacts on energy and water cycle: A review. *Global Planet. Change*, **112**, 79–91, doi:10.1016/j.gloplacha.2013.12.001.

Yao, T., Y. Wang, S. Liu, J. Pu, Y. Shen, and A. Lu, 2004: Recent glacial retreat in High Asia in China and its impact on water resource in northwest China. *Sci. China Earth Sci.*, **47**, 1065–1075.

Yao, Y., and B. Zhang, 2013: MODIS-based estimation of air temperature of the Tibetan Plateau. *J. Geogr. Sci.*, **23**, 627–640, doi:10.1007/s11442-013-1033-7.

You, Q., S. Kang, N. Pepin, W.-A. Flügel, Y. Yan, H. Behrawan, and J. Huang, 2010: Relationship between temperature trend magnitude, elevation and mean temperature in the Tibetan Plateau from homogenized surface stations and reanalysis data. *Global Planet. Change*, **71**, 124–133, doi:10.1016/j.gloplacha.2010.01.020.

——, K. Fraedrich, F. Sielmann, J. Min, S. Kang, Z. Ji, X. Zhu, and G. Ren, 2014: Present and projected degree days in China from observation, reanalysis and simulations. *Climate Dyn.*, **43**, 1449–1462, doi:10.1007/s00382-013-1960-0.

Zhu, X., O. Bothe, and K. Fraedrich, 2011: Summer atmospheric bridging between Europe and East Asia: Influences on drought and wetness on the Tibetan Plateau. *Quat. Int.*, **236**, 151–157, doi:10.1016/j.quaint.2010.06.015.